

The Influence of Different Rocks on Drillstring Stick-Slip Vibration

Changshuai Shi and Xin Du

Southwest Petroleum University, Chengdu Sichuan, 610500, China

Abstract

This paper establishes a torsional model of a two-degree-of-freedom drill string system composed of a rotary table and bottom-hole assembly, constructs a friction model between the drill bit and rocks, and considers the influence of five different rock types on the stick-slip vibration of the drill string system. The stick-slip vibration of the drill string system is analyzed under changes in top drive torque, top drive rotational speed, and weight on bit. The results show that different rocks cause varying degrees of stick-slip vibration due to their distinct friction coefficients: rocks with higher friction coefficients are more prone to induce stick-slip vibration. Meanwhile, increasing rotational speed and torque, as well as reducing weight on bit, can mitigate the impact of stick-slip vibration. This study provides assistance for systematic research on the influence of different rocks on drill string stick-slip vibration.

Keywords

Drillstring Systems; Stick-Slip Vibration; Rock Friction; Theoretical Modeling.

1. Introduction

Human survival and development rely heavily on vital natural resources such as petroleum and natural gas. However, with continuous exploitation, the development of shallow and medium-depth hydrocarbon resources in some regions has passed its peak. Consequently, future exploration and development will increasingly target deep and ultra-deep oil and gas fields[1][2]. As drilling depths increase, so do the associated risks. Therefore, enhancing drilling efficiency and safety necessitates in-depth research on drillstring systems. Drillstring mechanics has long been a focal point of research. Following extensive study and debate, the static analysis of drillstrings has become relatively well-established[3]. Current research emphasis has shifted towards dynamic analysis. The core of drillstring dynamics lies in vibrations and their control. The vibrations of the drillstring include unidirectional vibrations (axial, torsional, lateral), coupled vibrations (axial-torsional, lateral-torsional, axial-lateral, axial-torsional-lateral), and complex vibrations (stick-slip vibrations(SSV), drillstring whirl, etc.)[4]. Among these, SSV, as a particularly detrimental complex vibration, causes severe damage to the drillstring and bit, including premature component failure, excessive bit wear, and other detrimental effects. This significantly reduces tool life while simultaneously increasing drilling costs and safety hazards. Furthermore, increasing drilling depths lead to encounters with geologically complex formations exhibiting diverse lithologies. The friction characteristics of different rock types significantly influence the occurrence and severity of drillstring SSV. Therefore, investigating the influence of rock friction on SSV is crucial for optimizing drilling parameters during operations, ultimately improving drilling efficiency and reducing costs.

Stick-slip vibration manifests as a periodic alternation between the "stick" phase, where the bit is stationary and torque builds up, and the "slip" phase, where the bit suddenly rotates at a speed significantly higher than the top drive surface speed once the accumulated torque

exceeds the resisting torque at the bit. Numerous researchers have investigated SSV: Navarro-López et al[5] analyzed different nonlinear differential equations for modeling drillstring SSV, considering dry friction at the bit-rock interface. Brett[6] observed that a decrease in the speed of Polycrystalline Diamond Compact (PDC) bits can trigger SSV. Richard et al[7][8] studied SSV in drillstrings with drag bits, proposing that the velocity weakening effect is an inherent system characteristic, where minor perturbations can potentially induce SSV under specific conditions. Viguie et al[9] developed a passive vibration absorber to mitigate SSV through hardware solutions. Huang Zhiqiang et al[10] proposed a torsional model of a drill string system with four degrees of freedom to simulate impact drilling, concluding that torsional impact can mitigate stick-slip vibrations, prolong the service life of PDC bits, and improve drilling efficiency. Xiaoqiang Guo et al[11] used the finite element method to establish a nonlinear vibration model of drill string axial-torsional coupling, and studied the influence of feed rate and rotational drilling speed on the nonlinear behavior of drill string vibration. The results show that the axial vibration response of the drill string system exhibits an overall trend of quasi-periodic-chaotic transition with the increase of feed rate, and the torsional vibration of the drill string shows a periodic-chaotic trend. Saldivar et al[12] investigated the effects of drillstring surface rotational speed, torque, and weight on bit (WOB) forces. Zamanian et al[13] studied the self-excited SSV of a rotating drillstring with a drag bit, considering the top drive, mud damping, and an active damping system. Their results demonstrated that increasing drilling fluid damping, optimizing bit parameters, and selecting an appropriate active damping ratio can effectively suppress surface SSV.

Although research on stick-slip vibration has been relatively in-depth, it has not fully revealed the intrinsic mechanism by which complex lithology results in response differences of drill string stick-slip vibration. Under the background of continuous evolution of intelligent drilling systems, systematically analyzing how different rock properties differentially induce or affect stick-slip vibration is the key to improving system adaptability.

This study employs a Lumped Mass Model (LMM) for the drillstring system. Compared to alternative approaches such as Distributed Parameter Models or Neutral-Type Delay Models, the LMM offers distinct advantages for the analysis of drillstring dynamics pertinent to this investigation. Specifically, the LMM provides enhanced analytical tractability and facilitates a more concise formulation of the governing dynamic equations, significantly streamlining subsequent simulation. In this paper we established a two-degree-of-freedom (2-DOF) LMM representing the coupled dynamics of the top drive and the bottom-hole assembly (BHA), incorporating a friction model at the bit-rock interface. Simulations were conducted using Simulink to analyze the SSV behavior under varying operational parameters (top drive speed, torque, and Weight on Bit) for five distinct rock types: conglomerate(Cgl), limestone(Ls), phyllite(Phy), lithic sandstone(Lt.Ss), and pebbly coarse-grained quartz sandstone(P-Cg-Qtz Ss) with gravel. The findings from this systematic investigation provide critical insights into the differential influence of rock friction characteristics on drillstring SSV, thereby contributing to a deeper understanding of the phenomenon in geologically complex formations and offering valuable guidance for drilling parameter optimization.

2. Model Development

2.1. Simplified Torsional Vibration Model of the Drillstring System

Drilling in deep hard formations subjects the drillstring system—comprising drill pipes, the bit, and other downhole tools—to complex dynamics arising from its inherent properties, external excitations, and boundary conditions. Consequently, to facilitate mathematical analysis, a simplified model of the drillstring system is developed. Following the lumped parameter model definition by Márquez et al[14][15], the drillstring is conceptualized as a mass-spring-damper

system, governed by ordinary differential equations (ODEs). In essence, the drill pipes are represented as a linear torsional spring with stiffness k and torsional damping c . This leads to the establishment of a two-degree-of-freedom torsional model of the drillstring, as illustrated in Fig. 1, representing the coupled dynamics of the top drive and the bottom-hole assembly.

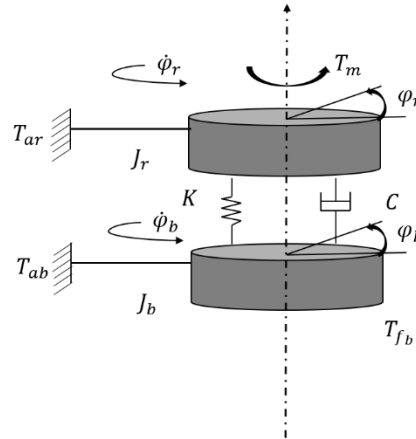


Fig 1. Two-Degree-of-Freedom Torsional Model of Drilling String

The two-degree-of-freedom torsional drillstring model described above was developed under the following key assumptions: (1) The drillstring system is situated in a vertical wellbore. (2) Only torsional vibration is considered; axial and lateral vibrations are neglected. (3) The effect of drilling fluid on the drillstring is modeled as an equivalent viscous damping. (4) Components of the drillstring system are abstracted and simplified into lumped mass-elastic elements.

Based on the model schematic shown in Fig. 1 the governing differential equations for the mass-spring-damper system are derived as follows:

$$\begin{cases} J_r \ddot{\varphi}_r + c(\dot{\varphi}_r - \dot{\varphi}_b) + k(\varphi_r - \varphi_b) = T_m - T_{ar} \\ J_b \ddot{\varphi}_b + c(\dot{\varphi}_b - \dot{\varphi}_r) + k(\varphi_b - \varphi_r) = -T_{fb} - T_{ab} \end{cases}$$

Where J_r is the rotational inertia of the top drive rotary table; J_b is the rotational inertia of the bottom hole assembly (BHA); k is the equivalent torsional stiffness coefficient between them; c is the equivalent damping coefficient between them; T_m is the torque provided by the rotary table; T_{fb} is the frictional torque at the drill bit; $\dot{\varphi}_r$ and $\dot{\varphi}_b$ are the angular velocities of the rotary table and the drill bit, respectively; $\ddot{\varphi}_r$ and $\ddot{\varphi}_b$ are the angular accelerations of the rotary table and the drill bit, respectively. Here:

$$T_{ar} = c_r \dot{\varphi}_r, \quad T_{ab} = c_b \dot{\varphi}_b$$

T_{ar} and T_{ab} are the damping torque on the top drive rotary table and the torque generated between the drill bit and the drilling fluid, respectively, with c_r and c_b being the damping coefficient of the top drive and the damping coefficient of the drilling fluid, respectively.

The above equation can be further simplified to:

$$\begin{cases} \ddot{\varphi}_r = \frac{1}{J_r} [\dot{\varphi}_r (-c - c_r) + c \dot{\varphi}_b - k(\varphi_r - \varphi_b) + T_m] \\ \ddot{\varphi}_b = \frac{1}{J_b} [\dot{\varphi}_b (-c - c_b) + c \dot{\varphi}_r - k(\varphi_b - \varphi_r) + T_{fb}] \end{cases}$$

Selecting $\omega_r = \dot{\varphi}_r$, $\omega_b = \dot{\varphi}_b$, and $\Delta\varphi = \varphi_r - \varphi_b$ as the state variables, and assuming constant rotary speed and weight on bit (WOB), the above equation can be rewritten as:

$$\begin{cases} \dot{\omega}_r = -\frac{c+c_r}{J_r}\omega_r + \frac{c}{J_r}\omega_b - \frac{k}{J_r}\Delta\varphi + \frac{1}{J_r}T_m \\ \dot{\omega}_b = \frac{c}{J_b}\omega_r - \frac{c+c_b}{J_b}\omega_b + \frac{k}{J_b}\Delta\varphi - \frac{1}{J_b}T_{fb} \\ \Delta\dot{\varphi} = \omega_r - \omega_b \end{cases}$$

2.2. Friction Model between Bit and Rock

Typical friction models used to describe frictional behavior include the Coulomb friction model, the Stribeck friction model, and the Karnopp friction model[16]. Among these, the Stribeck and Karnopp friction models are frequently employed in the study of stick-slip vibrations. This paper adopts the Karnopp model. In this model, the friction force f is a function of the relative sliding velocity. Within a defined small velocity interval $[-D_v, D_v]$, the velocity is approximately considered to be zero ($D_v = 0$), and the object is assumed to be in a sticky state. In this state, the magnitude of the friction force is determined by the external force acting on the system. When the velocity exceeds this interval, the friction force is considered to be dependent on the magnitude of the velocity. The expression for the model is given as follows:

$$T_{fb} = \begin{cases} T_{eb}(x) & \text{if } |\dot{\varphi}_b| < D_v, |T_{eb}| \leq T_{sb} \\ T_{sb} \operatorname{sgn}(T_{eb}(x)) & \text{if } |\dot{\varphi}_b| < D_v, |T_{eb}| > T_{sb} \\ T_{cb}(x) \operatorname{sgn}(\dot{\varphi}_b) & \text{if } |\dot{\varphi}_b| \geq D_v \end{cases}$$

$$T_{sb} = \mu_{sb} W_{ob} R_b$$

$$T_{eb}(x) = c(\dot{\varphi}_r - \dot{\varphi}_b) + k(\varphi_r - \varphi_b) - T_{ab}$$

$$T_{cb} = R_b W_{ob} \mu_b(\dot{\varphi}_b)$$

$$\mu_b(\dot{\varphi}_b) = \mu_{cb} + (\mu_{sb} - \mu_{cb}) e^{-\gamma_b |\dot{\varphi}_b| / v_f}$$

Where T_{eb} is the driving torque on the drill bit; T_{sb} is the maximum static friction torque between the drill bit and rock; μ_{sb} and μ_{cb} are the static friction coefficient and the Coulomb friction coefficient, respectively; W_{ob} is the weight on bit; R_b is the radius of the drill bit; D_v is the boundary layer thickness; γ_b is a constant defining the velocity decline rate of T_{fb} ; v_f is an empirical constant.

3. Analysis of the Influence of Different Rock Types on Stick-Slip Vibration in Drillstring Systems

3.1. Influence of Top Drive Speed Variation on Drillstring Stick-Slip Vibration

Table 1. Friction Coefficients of Different Rock Types[17]

Rock Types	μ_{sb}	μ_{cb}
Phy	0.42	0.38
Ls	0.53	0.58
Lt.Ss	0.47	0.47
Cgl	0.87	0.55
P-Cg-Qtz Ss	1.07	0.59

During the drilling process, different rock types, with their distinct static and dynamic friction coefficients, lead to varying manifestations of stick-slip vibration in the drillstring. This study investigates five different rock types, and their specific friction coefficient values are listed in Table 1.

Table 2. Simulation Parameters[18]

Parameter	Symbol	Magnitude
Moment of inertia of the top drive	J_r	2122 kg·m ²
Moment of inertia of bottom hole assembly (BHA)	J_b	374 kg·m ²
Equivalent damping coefficient of drill string	c	23.2 Nms/rad
Equivalent stiffness coefficient of drill string	k	473 Nm/rad
Boundary layer thickness	D_v	1e-6
Bit radius	R_b	0.155575
Weight on bit	W_{ob}	97347
Top drive damping coefficient	c_r	425
Bit damping coefficient	c_b	50
A constant defining the rate of decrease of velocity T_{fb}	γ_b	0.9
An empirical constant	v_f	1

Fig 2 shows the drill bit rotational speed curves under different conditions. The results indicate that different rock types, due to their inherent differences in static and dynamic friction coefficients, directly affect the downhole force conditions and the torsional response of the drillstring. Consequently, under different top drive angular velocities, the drill bit's angular velocity exhibits distinct dynamic characteristics. As the top drive speed increases, the maximum rotational speed attainable by the drill bit during drilling shows a clear upward trend. At top drive speeds of $\omega_r = 5$ rad/s and $\omega_r = 10$ rad/s, typical stick-slip vibration occurs when drilling in Cgl; and P-Cg-Qtz Ss, which have higher friction coefficients. This phenomenon is characterized by periodic, severe fluctuations in the drill bit speed, frequently manifesting as a "zero-speed stall followed by a sudden high-speed spike." This is attributed to the significant difference between the static and dynamic friction coefficients of these rocks, which readily triggers a cycle of "storage and release" of torsional energy in the drillstring. In contrast, no stick-slip vibration is observed when drilling in other rocks with relatively lower friction coefficients, such as Ls, Phy, and Lt.Ss. For these rocks, the difference between static and dynamic friction coefficients is smaller. The drill bit speed exhibits only minor initial oscillations due to transient force imbalance between the drillstring and the bottom hole, subsequently stabilizing as the drillstring torque and the bottom hole reaction force gradually reach a dynamic equilibrium.

Furthermore, by comparing the specific variations in drill bit speed at $\omega_r = 5$ rad/s and $\omega_r = 10$ rad/s (e.g., the maximum speed in Cgl is approximately 16.34 rad/s at $\omega_r = 5$ rad/s, rising to

over 23 rad/s at $\omega_r = 10$ rad/s), it can be clearly concluded that as ω_r increases, the maximum rotational speed achieved by the drill bit during drilling also increases, regardless of whether stick-slip vibration occurs in the formation.

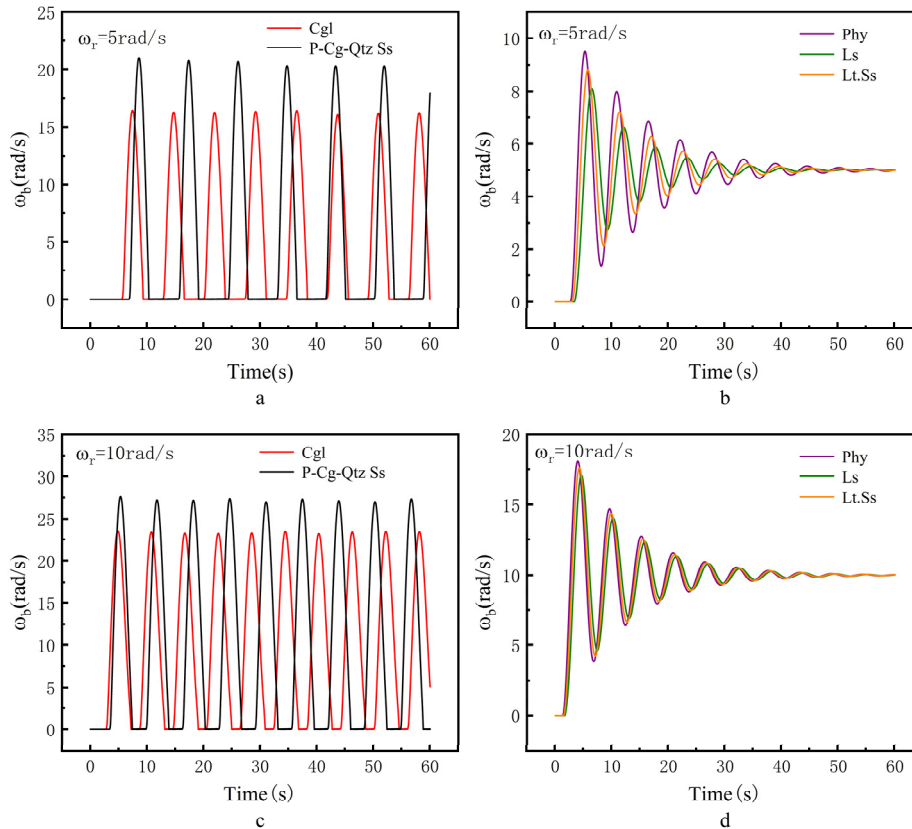


Fig 2. Drill Bit Rotational Speed Curves at $\omega_r = 5$ rad/s and 10 rad/s

Fig 3 illustrates the variation in drill bit rotational speed when drilling in five different rock types at a top drive speed of 20 rad/s. The results show that when the top drive speed is increased to this operational condition, no stick-slip vibration occurs during drilling in any of the five rock types.

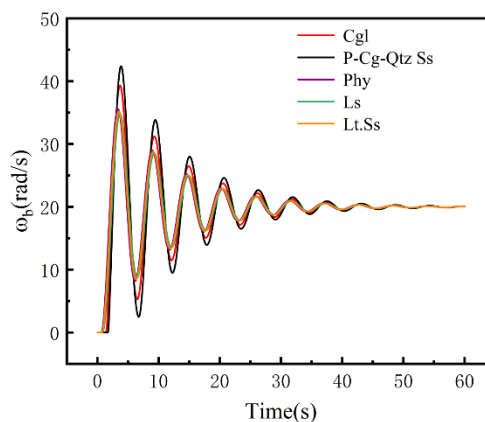


Fig 3. Drill Bit Rotational Speed Curves at $\omega_r = 20$ rad/s

From the perspective of the curves' dynamic behavior, at the initial moment, the drill bit speed rapidly responds from zero to the torsional driving force from the top drive. Subsequently, the speed curves for each lithology enter a brief phase of oscillation. The curves for Cgl and P-Cg-

Qtz Ss exhibit relatively larger oscillation amplitudes, while those for Phy, Ls, and Lt.Ss show gentler fluctuations. However, in none of the cases does the drill bit speed enter a "zero-speed stall" state. As time progresses, the oscillation amplitudes of all curves gradually diminish, and the drill bit speeds for the different lithologies progressively stabilize. The core mechanism behind this phenomenon is that when the top drive speed is increased to 20 rad/s, the continuous torsional driving force it transmits to the drillstring is significantly enhanced.

3.2. Influence of Top Drive Torque on Drillstring Stick-Slip Vibration

As a core parameter of drillstring torsional drive, the dynamic variation of top drive torque plays a crucial role in regulating stick-slip vibration. Fig 4 shows the variation curves of top drive speed and drill bit speed over time under a constant top drive torque of 4000 N·m. It can be observed from the figure that under this condition, no stick-slip vibration occurs in the drillstring system while drilling in any of the five rock types. The provided driving torque at this level is sufficient to overcome the friction torque at the drill bit-rock interface, preventing the system from entering a stuck state. Consequently, the drill bit maintains continuous rotation, and its speed does not drop to zero.

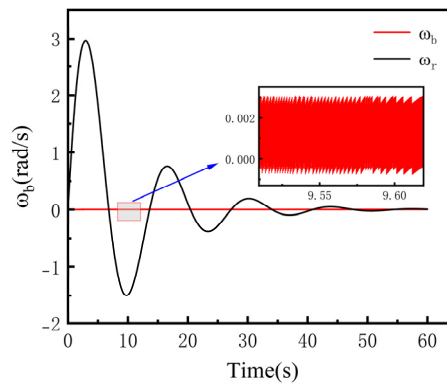


Fig 4. Variation Curves of Top Drive Speed and Drill Bit Rotational Speed over Time under a Constant Top Drive Torque of 4000 N·m

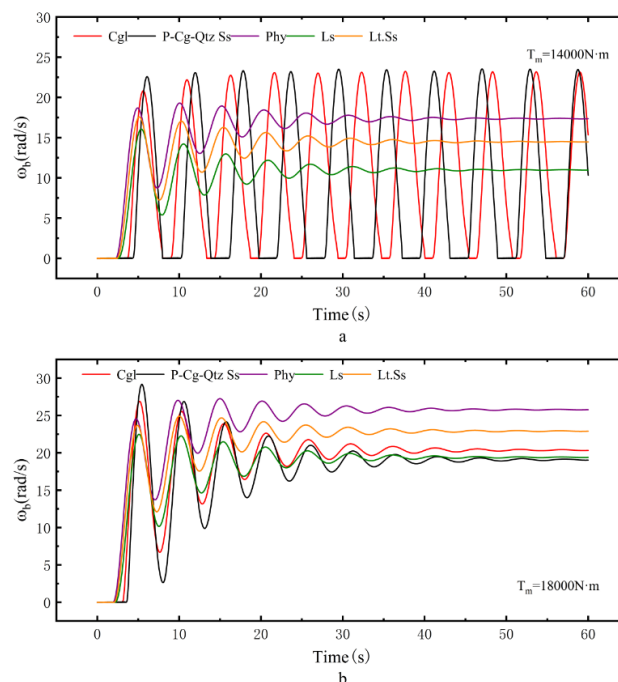


Fig 5. Variation of Drill Bit Rotational Speed under Different Top Drive Torques ($T_m = 14,000$ and $18,000$ N·m)

As the top drive torque is further increased, the variation over time is shown in Fig 5. It can be observed from the figure that at $T_m = 14,000$ N·m, pronounced and severe periodic fluctuations occur only for rocks with higher friction coefficients, such as Cgl and P-Cg-Qtz Ss. This observation aligns with the previously established pattern that rocks with high friction properties are prone to inducing stick-slip vibration. Under this torque condition, rocks with lower friction coefficients, namely Phy, Ls, and Lt.Ss, exhibit no stick-slip vibration. When the torque is further increased to $T_m = 18,000$ N·m, stick-slip vibration ceases to occur in all rock types. The drill bit speed undergo a period of oscillation before eventually stabilizing at steady-state values.

3.3. Influence of Weight on Bit on Drillstring Stick-Slip Vibration

Following the analysis in the preceding two subsections on the governing mechanisms of stick-slip vibration by the driving-end parameters—namely, top drive speed and torque—the influence of Weight on Bit (WOB) cannot be overlooked. As a core load parameter acting directly on the drill bit-rock interface at the bottom hole, WOB plays a significant role in the occurrence and characteristics of stick-slip vibration. In this section, with all other parameters held constant, the Weight on Bit was varied. The specific WOB values used are listed in Table 3.

Table 3. The specific WOB values used are listed

	WOB 1	WOB 2	WOB 3
Magnitude	37347 N	57347 N	77347 N

Fig 6 illustrates the variation of drill bit rotational speed over time when drilling in five different rock types under different WOB conditions, clearly revealing the correlation mechanism between WOB and stick-slip vibration.

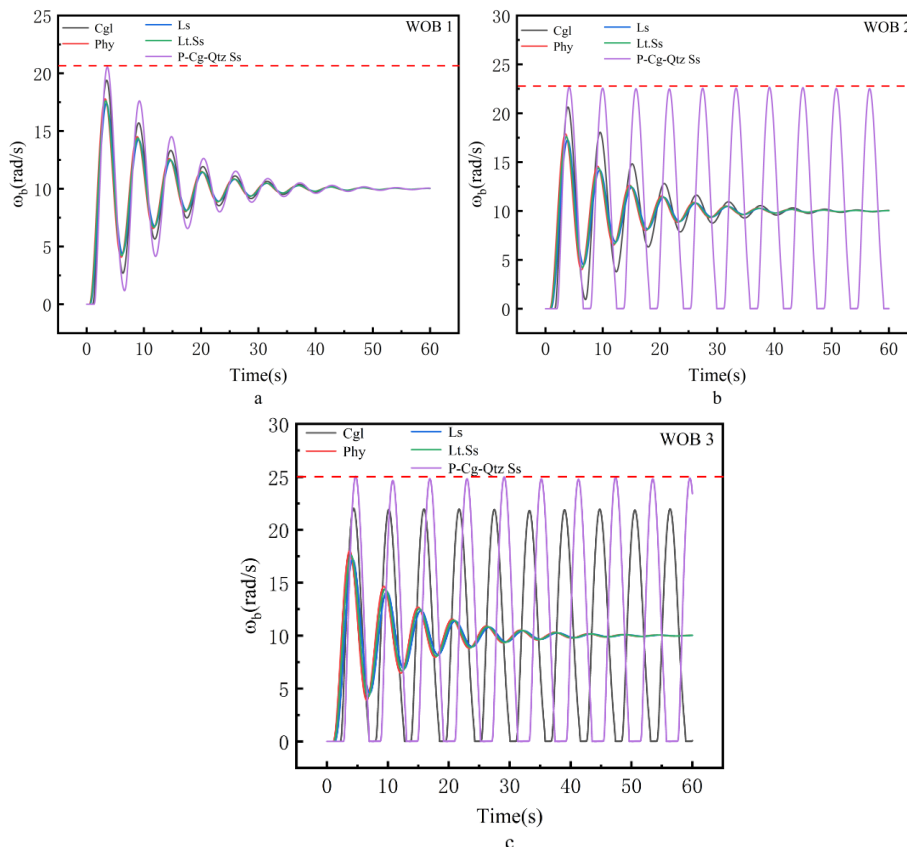


Fig 6. Variation of Drill Bit Rotational Speed under Three Different Weights on Bit.

Under WOB 1 (as shown in Fig a), all five rock types exhibit severe fluctuations during the initial stage (0–35 s). After 35 s, these oscillations gradually diminish and eventually stabilize. Notably, the oscillation range is relatively smaller for rocks with lower friction coefficients, such as Phy, Ls, and Lt.Ss, while it is larger for rocks with higher friction coefficients, namely Cgl and P-Cg-Qtz Ss. When the WOB is increased to Condition 2 (Fig b), stick-slip vibration emerges for P-Cg-Qtz Ss. This occurs because a higher WOB requires the drillstring to accumulate greater torsional energy to overcome the increased frictional torque at the bit-rock interface. Rocks with higher friction coefficients require proportionally more energy to overcome this torque under increased WOB. Under WOB 3 (Fig c), stick-slip vibration also occurs in Cgl, further demonstrating that increasing WOB can induce or intensify stick-slip vibration in the drillstring. Comparing Conditions 2 and 3, the maximum rotational speed for P-Cg-Qtz Ss increases from approximately 22.5 rad/s to 24.8 rad/s. This indicates that as WOB increases, the peak speed during stick-slip vibration also rises.

Fig 7 shows the variation of the torque difference ($T_m - T_{fb}$) over time under different WOB conditions. In Fig 7a (WOB 1), the $T_m - T_{fb}$ values for all rock types remain positive. After a period of oscillation, they stabilize. Even for rocks with higher friction coefficients, such as P-Cg-Qtz Ss and Cgl, $T_m - T_{fb}$ does not become negative, indicating the absence of stick-slip vibration. This observation aligns with the results shown in Fig 7a.

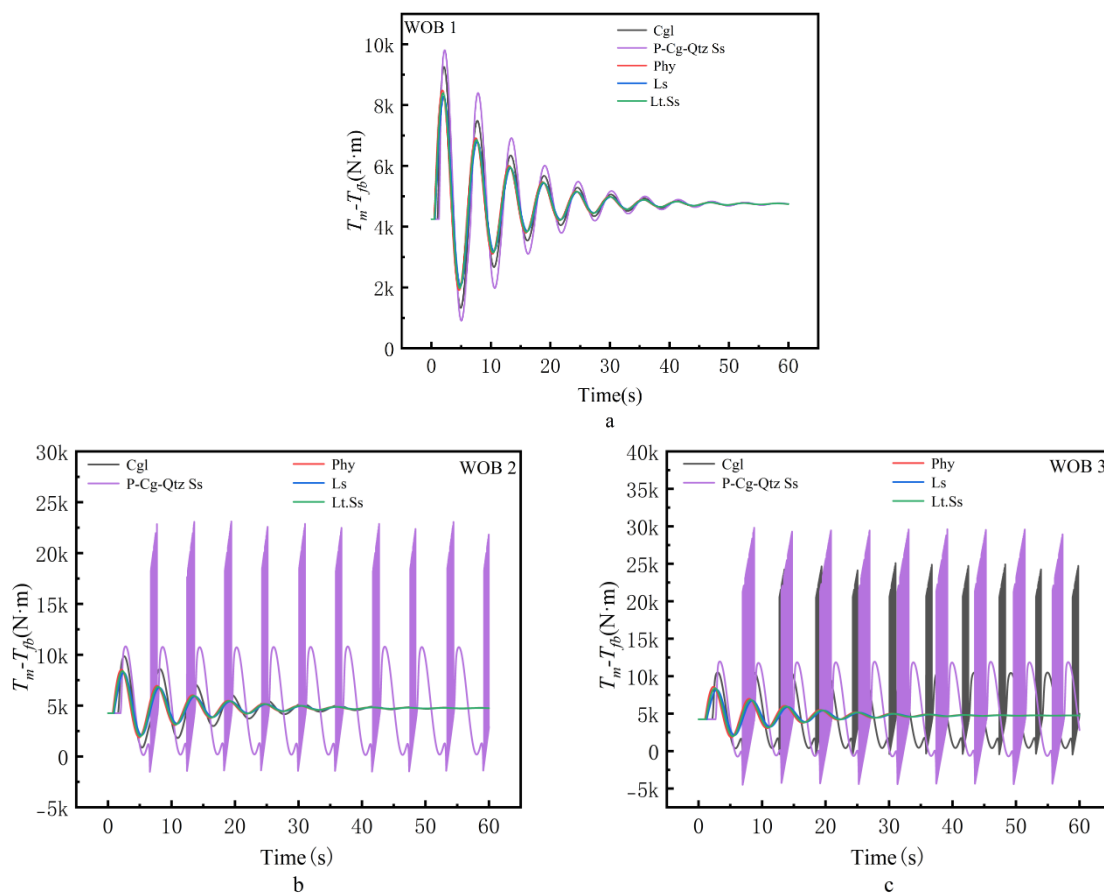


Fig 7. Variation of the $T_m - T_{fb}$ under Different Weights on Bit

When the WOB is increased to Condition 2 (Fig 7b), Phy, Ls, Lt.Ss, and Cgl still show no stick-slip vibration, with $T_m - T_{fb}$ remaining positive. However, for P-Cg-Qtz Ss, $T_m - T_{fb}$ periodically becomes negative, accompanied by large-amplitude, cyclic oscillations. This signifies that under

WOB Condition 2, the frictional torque at the bit-rock interface in this rock type can exceed the top drive torque. The drillstring then enters a stuck state and begins to accumulate torsional energy until $T_m - T_{fb}$ becomes positive again. The severe fluctuations of $T_m - T_{fb}$ in Fig 7b also explain why, in the corresponding speed curve, the drill bit speed surges to more than twice its stable value upon transitioning from the stick phase to the slip phase.

Under WOB 3 (Fig 7c), both Cgl and P-Cg-Qtz Ss exhibit intense periodic oscillations with intervals of negative $T_m - T_{fb}$. This demonstrates that a further increase in WOB can induce stick-slip vibration in rocks with relatively higher friction coefficients. Therefore, in practical drilling operations, adjusting the applied WOB based on the specific lithology encountered can be an effective strategy to mitigate stick-slip vibration.

4. Conclusion

This study investigates the influence of different rock types on stick-slip vibration in drillstring systems by establishing a two-degree-of-freedom drillstring dynamics model and a bit-rock friction model. The analysis is conducted from three perspectives: varying the top drive speed, the top drive torque, and the weight on bit.

The results indicate that under a constant torque and variable speed condition, stick-slip vibration occurs when drilling through Cgl and P-Cg-Qtz Ss at top drive speeds of 5 rad/s and 10 rad/s, whereas no such vibration is observed in Lt.Ss, Ls, or Phy. Furthermore, rocks with higher friction coefficients correspond to greater maximum achievable angular velocities of the drill bit and higher maximum torque on the rotary table. However, when the top drive speed is increased to 20 rad/s, stick-slip vibration is suppressed in all five rock types.

Under a constant speed and variable torque condition, no stick-slip vibration occurs in any of the rock types at a relatively low torque. As the applied torque increases, rocks with higher friction coefficients become more susceptible to stick-slip vibration. Similarly, under different WOB conditions, an increase in WOB makes rocks with higher friction coefficients more prone to stick-slip vibration.

References

- [1] Li, L., Hao, H., Bai, X., Li, B. Stick-slip vibration analysis of a coupling drilling-rock system with two delays and one delay-dependent coefficient. *Chaos, Solitons & Fractals* 2024, 186.
- [2] H, X, Song., J, X, Guo., J, Li., S, L, Zhang., Oliveira, A. J. S. de., He, A. G. Application of multifunctional wellbore cleaning fluid in the removal of residual drilling fluids in ultra-deep wells: Research progress and prospects. *Geoenergy Science and Engineering* 2024, 243.
- [3] Z, F, Li., C, Y, Zhang., G, M, Song. Research advances and debates on tubular mechanics in oil and gas wells. *Journal of Petroleum Science and Engineering* 2017 151, 194-212.
- [4] Song, J. Z., Liu, S., He, Y. F., Jiang, S. X., Zhou, S. G., Zhu, H. J. The state-of-the-art review on the drill pipe vibration. *Geoenergy Science and Engineering* 2024, 243.
- [5] Navarro-Lopez.E.M., Suarez.R. Practical approach to modelling and controlling stick-slip oscillations in oilwell drillstrings. *Proceedings of the 2004 IEEE International Conference on Control Applications, Taipei, Taiwan (2004)*, p. 1454-1460.
- [6] BRETT J F. The genesis of torsional drilling vibrations. *SPE Drilling Engineering* (1992), 7, 168-174.
- [7] RICHARD T, GERMAY C, DETOURNAY E. Self-excited stick-slip oscillation of drill bits. *Comptes Rendus Mecanique* (2004), 332, 619-626.
- [8] RICHARD T, GERMAY C, DETOURNAY E. A simplified model to explore the root cause of stick-slip vibration in drilling systems with drag bits. *Journal of Sound and Vibration* (2007), 305, 432-456.

- [9] Vigui.R., Kerschen.G., Golinval, J.C., McFarland, D.M., Bergman, L.A., & Vakakis, A.F., Wouw f.N.V.D. Using passive nonlinear energy transfer to stabilize drill-string systems. *Mechanical Systems and Signal Processing* (2009), 23, 148-169.
- [10] Zhiqiang, Huang., Dou, Xie., Bing, Xie., Wenlin, Zhang., Fuxiao, Zhang., Lei, He. Investigation of PDC bit failure base on stick-slip vibration analysis of drilling string system plus drill bit. *Journal of Sound and Vibration* (2018), 417, 97-109.
- [11] Xiaoqiang, Guo., Zhichen, Qiu., Mingming, Li., Xinye, Li., Ning, Hu., Libin, Zhao., Chengyang, Ye. Axial-torsional coupling vibration model and nonlinear behavior of drill string system in oil and gas wells. *Communications in Nonlinear Science and Numerical Simulation* (2025), 142.
- [12] Saldivar., Belem., Sabine, Mondié., Juan-Carlos, Avila-Vilchis. The control of drilling vibrations: A coupled PDE-ODE modeling approach. *International Journal of Applied Mathematics and Computer Science* (2016), 26, 335-349.
- [13] M, Zamanian., S.E, Khadem., M.R, Ghazavi. Stick-slip oscillations of drag bits by considering damping of drilling mud and active damping system. *Journal of Petroleum Science and Engineering* (2007), 59, 289-299.
- [14] Saldivar, Márquez., M, B., Boussaada, I., Mounier, H., Niculescu, SI. An Overview of Drillstring Models. In: *Analysis and Control of Oilwell Drilling Vibrations. Advances in Industrial Control* (2015). Springer, Cham.
- [15] Jasem, M, Kamel., Asan, G.A, Muthalif., Abdulazim, H, Falah. A review of vertical drill-string mathematical modelling. *Applications in Engineering Science* (2025), 22.
- [16] Wang, Q., Zhang, Q., Wang, Z., Mo, J., Jin, W., & Zhu, S. Identification of Stribeck Model Parameters to Accurately Reveal Stick-Slip Characteristics of a Disc-Block Friction System. *Tribology Transactions*, (2023), 66(6), 1026-1042.
- [17] Han, W. Frictional sliding characteristics of rocks and analysis of its influencing factors (Doctoral dissertation, Taiyuan University of Technology, China, (2012), p. 48-49.
- [18] J. D, Jansen., L, van den Steen. Active Damping of Self-excited Torsional Vibrations in Oil Well Drillstrings. *Journal of Sound and Vibration*. (1995), 179, 647-668.